Automatic regulatory control in type 1 diabetes without carbohydrate counting☆

Patricio Colmegna [a,d], Fabricio Garelli [b,d], Hernán De Battista [b,d], Ricardo Sánchez-Peña [c,d,*]

[a] Universidad Nacional de Quilmes, Roque Sáenz Peña 352, 1876, Buenos Aires, Argentina
[b] Universidad Nacional de La Plata, Calle 48 y 116, CC 91, 1900, Buenos Aires, Argentina
[c] Instituto Tecnológico de Buenos Aires, Av. Eduardo Madero 399, 1106, Buenos Aires, Argentina
[d] CONICET, Godoy Cruz 2290, 1425, Buenos Aires, Argentina

ARTICLE INFO

Keywords:
Artificial pancreas
Glucose control
Switched LQG control
Sliding mode control
Insulin on board

ABSTRACT

A new approach to automatically regulate the glucose level in type 1 diabetes is presented in this work. This is the so-called Automatic Regulation of Glucose (ARG) algorithm, which is based on a switched Linear Quadratic Gaussian (LQG) inner controller, combined with an outer sliding mode safety loop with Insulin on Board (IOB) constraints. *In silico* and *in vivo* results without feedforward insulin boluses delivered at meal times indicate that safe blood glucose control can be achieved by the proposed controller. This controller is simple to migrate to well-known hardware platforms, and intuitive to tune using *a priori* clinical information.

1. Introduction

Type 1 Diabetes Mellitus (T1DM) is a disease characterized by the inability to produce insulin, due to the destruction of the pancreatic β-cells. Insulin deficiency generates chronic hyperglycemia that can be related to several health complications, like the acceleration of atherosclerosis (Chait & Bornfeldt, 2009). In order to regulate their glucose levels, patients have to be continuously measuring their glycemia, and calculating how much insulin they need, making T1DM an extremely demanding disease. On the other hand, Insulin Intensive Treatment (IIT) is also associated with an increase risk of hypoglycemia (The Diabetes Control and Complications Trial Research Group, 1997).

An Artificial Pancreas (AP) is a system that automatically modulates patient's insulin infusion rate in order to maintain his/her blood glucose within safe limits. Although intravenous AP is possible (Renard, 2008), both measurement and infusion are, in general, performed subcutaneously via a Continuous Glucose Monitoring (CGM) sensor, and a Continuous Subcutaneous Insulin Infusion (CSII) pump, respectively. This represents a minimally invasive AP scheme that allows ambulatory use, but unfortunately, makes the control problem much harder. Amongst other difficulties, lag-times and errors in glucose measurement and insulin action, nonlinearities, large dynamic uncertainties and technical difficulties (sensor dropouts and insulin set failure) have to be coped with (see Bequette (2012) and Steil, Panteleon, and Rebrin (2004) for a complete review of the challenges in the development of an AP system). It is worth remarking that even rapid-acting insulin introduces a significant delay that affects the performance of a glucose controller (Steil et al., 2004). Actually, this is the main limitation for AP systems, considering that according to pharmacodynamics profiles the peak of insulin action occurs about 70 min after infusion (Walsh, Roberts, & Heinemann, 2014).

The AP development has been accelerated by the use of elaborated simulators, such as the UVA/Padova metabolic simulator which was accepted by the US Food and Drug Administration (FDA) in lieu of animal trials (Kovatchev, Breton, Dalla Man, & Cobelli, 2008, 2009). Recently, clinical trials were performed in different countries of the EU, USA, Israel and Australia (de Bock et al., 2015; Gondhalekar, Dassau, & Doyle III, 2016; Hovorka et al., 2014; Phillip et al., 2013). The great majority of the control algorithms that have been clinically tested are based on Proportional-Integral-Derivative (PID), Model Predictive Control (MPC) or fuzzy logic controllers. Generally, they are hybrid (semi-automatic) control loops, where the controller action is complemented with premeal insulin boluses in both the single-hormone (Bally et al., 2017; Forlenza et al., 2017; Kovatchev et al., 2017; Ly et al., 2015; Messori et al., 2017) and the dual-hormone (El-Khatib et al., 2017; Haidar, Messier, Legault, Ladouceur, & Rabasa-Lhoret, 2017) AP. Although the injection of an open-loop bolus based on the carbohydrate intake facilitates the reduction of postprandial glucose values (Weinzimer

☆ Research in this area is partially supported by Nuria/Cellex Foundations, by the Argentinian government (MINCYT PICT 2014-2394, CONICET PIP 112-201501-00837 CONICET, UNLP 11/I216), and the EU (ERANET ELAC 2015/T09-103).
* Corresponding author at: Instituto Tecnológico de Buenos Aires, Av. Eduardo Madero 399, 1106, Buenos Aires, Argentina.
E-mail address: rsanchez@itba.edu.ar (R. Sánchez-Peña).

et al., 2008), inaccurate carbohydrate counting is frequent (Brazeau et al., 2013). In El-Khatib et al. (2017) meal announcement is not required, but it is suggested in order to trigger a meal-priming bolus based on a meal size classification akin to the proposal of Gingras, Haidar et al. (2016) and Gingras, Rabasa-Lhoret et al. (2016).

Studies involving fully closed-loop AP systems can be found in Dassau et al. (2013), Steil, Rebrin, Darwin, Hariri, and Saad (2006) and more recently in Blauw, van Bon, Koops, DeVries, and on behalf of the PCDIAB consortium (2016), Cameron et al. (2017), Reddy et al. (2015) and Turksoy et al. (2017). Despite promising results, there is still a strong compromise between the aggressiveness of the control action and the postprandial glucose excursion. This compromise exists even when meals can be anticipated based on a probabilistic approach like the one presented in Cameron, Niemeyer, and Bequette (2012). If the controller is not aggressive enough to a meal perturbation, then prolonged hyperglycemia may occur (Reddy et al., 2015; Weinzimer et al., 2008). On the other hand, if the controller is too aggressive, there is a higher risk of insulin overdosing, and consequently, postprandial hypoglycemia (Cameron et al., 2017). The latter is partially because the effect of the meal on the CGM signal is not immediate, and therefore, the insulin response generated by the controller to cope with the meal is delayed several minutes. It should also be considered that in the standard open-loop basal-bolus treatment, a unique insulin bolus is applied at meal times. Instead, in a feedback control scheme, multiple insulin boluses are generated in response to the change in the CGM signal. Furthermore, because the counter-regulatory response in people with T1DM is often compromised, the response of an AP control algorithm should be less aggressive than the β-cell's secretory response (Steil et al., 2004). As a consequence, fully closed-loop systems have an increased risk of initial hyperglycemia and late hypoglycemia during meals in comparison with semi-automated hybrid strategies. In Turksoy et al. (2017), this problem is reduced, because the insulin bolus to cover the meal is not generated by the multivariable adaptive controller *per se*, but by an additional module that infuses an insulin bolus when a meal is detected.

In this paper, relatively unexplored control techniques in the field are proposed to address the glucose control paradigm, and take a step forward towards a fully automatic control loop. In particular, a couple of Linear Quadratic Gaussian (LQG) controllers are employed as main feedback controllers in combination with a sliding-mode safety layer to include Insulin on Board (IOB) constraints. Both LQG controllers are arranged into a switched structure to cope with the trade-off between prandial and fasting periods by triggering the controller into an *aggressive* mode during meals. The combination of the switched LQG controller with the safety mechanism allows to compensate for delays associated with subcutaneous insulin infusion. When the *aggressive* mode is triggered, an insulin spike is generated. This mimics the first-phase insulin secretion of the β-cell response (Steil et al., 2004). On the other hand, the purpose of the safety layer is to reduce the insulin infusion commanded by the switched LQG controller when a predefined IOB limit is going to be violated. This latter characteristic can be associated with the suppression of the β-cell in proportion to plasma insulin levels (Steil et al., 2004). In this way, an initial "under-damped" insulin response can be generated to compensate for insulin delays, without increasing the risk of postprandial hypoglycemia. It is worth remarking that here it is the first time the safety layer is employed to adapt a closed-loop control without premeal insulin boluses.

The proposed control structure also intends to simplify both controller tuning and implementation. This facilitated its *in vivo* validation in a clinical trial, where it was tested on five T1DM adults during 36 h without carbohydrate counting. This was the second phase of the first AP clinical trial campaign in Latin America. In the first phase a hybrid controller was tested in the same site and by the same team (Sánchez-Peña et al., 2017).

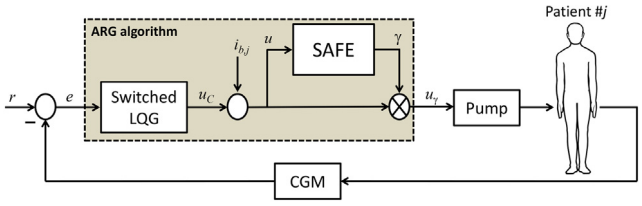

Fig. 1. Closed-loop system with the ARG algorithm, where $i_{b,j}$ is the patient-specific basal rate, and r is the reference glucose concentration.

2. Control algorithm

Automatic feedback control of the blood glucose levels has several opposing requirements, e.g., CGM noise immunity and fast response for meal perturbations. These are difficult to achieve with a single Linear Time Invariant (LTI) controller, and motivates the design of a multicontroller structure (Colmegna, Sánchez-Peña, Gondhalekar, Dassau, & Doyle III, 2016b; Gondhalekar, Dassau, & Doyle III, 2014). In this work, the main controller is defined as a multicontroller structure that switches between two LQG controllers. A conservative controller performs slight changes on the patient's basal insulin infusion rate, and an aggressive one is selected at the time of meal ingestion to rapidly generate an insulin spike, and as a consequence, reduce postprandial hyperglycemia risks. In order to obtain a simple controller structure that provides stability guarantees, the multicontroller is arranged into the framework presented in Hespanha and Morse (2002).

A schematic of the closed-loop system with the Automatic Regulation of Glucose (ARG) algorithm is presented in Fig. 1. As shown in that figure, the ARG algorithm is also composed of a Safety Auxiliary Feedback Element (SAFE) layer that adds a second degree-of-freedom to the switched LQG, as it quickly adapts (reduces) the insulin infusion when a given constraint on the residual insulin (or IOB) is reached. Thus, the response of the multicontroller can be shaped with the SAFE mechanism in order to obtain a closed-loop insulin infusion rate akin to a basal-bolus strategy. That is, no feedforward action such as meal boluses is required, which significantly increases the autonomy of the glucose control system, and of the patient. In addition, the activation of the SAFE layer can also be employed to switch amongst the aggressive and conservative LQG controllers.

In the following subsections the analysis and design of the control algorithm are detailed.

2.1. Switched LQG control

The multicontroller is synthesized using a control-oriented model recently developed by our group that is based on the adult cohort of the distribution version of the UVA/Padova simulator (Colmegna, Sánchez-Peña, & Gondhalekar, 2018).

Patient design model

The idea behind this model is simple, and can be summarized as follows. First, a general LTI low-order model from the subcutaneous-insulin delivery input (pmol/min) to the subcutaneous-glucose concentration deviation (mg/dl) is proposed:

$$G(s) = k\frac{s+z}{(s+p_1)(s+p_2)(s+p_3)}e^{-15s}. \tag{1}$$

This model is inspired on previous control-oriented ones that have shown effectiveness to synthesize diverse control strategies (Colmegna et al., 2016b; Lee, Dassau, Seborg, & Doyle III, 2013; van Heusden, Dassau, Zisser, Seborg, & Doyle III, 2012). Then, an average Linear Parameter-Varying (LPV) model is constructed by making the parameter p_1 of model (1) be a function of the glucose level g, which can be measured in real time. The procedure to compute p_1 as a function of

Table 1
Model comparison in terms of the NRMSE. Increase is over the proposed personalized LTI control-oriented model.

Model	[70–180] mg/dl		[40–400] mg/dl	
	Average NRMSE	Increase (%)	Average NRMSE	Increase (%)
Proposed Personalized LTI model	0.1067	0	0.2128	0
Model presented in van Heusden et al. (2012)	0.2055	92.6	0.2283	7.3
Model presented in Colmegna, Sánchez-Peña, Gondhalekar, Dassau, and Doyle III (2016a)	0.3447	223.1	0.3256	53.0
Model presented in Lee et al. (2013)	0.1919	79.9	0.3266	53.5

g is detailed in Colmegna et al. (2018). Basically, the dependence of p_1 on g allows representing the time-varying nature of the insulin-glucose system. In this simple manner of replicating the T1DM dynamics, model parameters are fixed and equal to $z = 0.1501$, $p_2 = 0.0138$ and $p_3 = 0.0143$ for all patients. Finally, the last step consists in tuning the model's gain k using the patient's Total Daily Insulin (TDI) by means of the so-called 1800 rule (1800/TDI), which is an insulin sensitivity factor. Therefore, for each patient #j a personalized k_j is obtained. In this way, the interpatient variability can be represented using *a priori* clinical information that is easily obtainable and extensively used in clinical care. In addition, it is worth mentioning that the proposed personalized LPV model can lead to straightforward LPV controller design, because it is affine in the time-varying parameter p_1.

Although successful results in T1DM control were obtained with LPV controllers (Colmegna et al., 2016a, b; Szalay, Eigner, & Kovács, 2014), a simpler LQG control strategy is proposed in this work. From the implementation point of view, an LQG approach is more intuitive to tune and easier to migrate into a portable platform like the Diabetes Assistant (DiAs) system (Keith-Hynes, Mize, Robert, & Place, 2014), which is the AP research platform selected for these trials. Hence, in order to synthesize LQG controllers, the LTI model resulting by holding the glucose-varying parameter $p_1(g)$ of the personalized LPV model fixed at $p_1^* = p_1(120)$ is considered. The glucose concentration $g = 120$ mg/dl is the closed-loop reference, and therefore, the glucose level approximately reached at closed-loop without external perturbations (Dalla Man et al., 2014). Thus, the following control-oriented LTI model:

$$\mathcal{G}_j(s) = k_j \frac{s+z}{(s+p_1^*)(s+p_2)(s+p_3)} \mathrm{e}^{-15s} \tag{2}$$

is assigned for each T1DM adult #j. In this case, the time-varying nature of the system is considered through the switched LQG controller.

In order to present model validation results, the comparison procedure presented in Colmegna et al. (2018) is repeated here, considering model (2) and the control-oriented LTI models presented in Colmegna et al. (2016b), Lee et al. (2013) and van Heusden et al. (2012). The procedure is as follows. For each adult patient of the distribution version of the UVA/Padova metabolic simulator at each particular steady-state glucose concentration (operating point), the Root Mean Square Error (RMSE) between the time-response of each control-oriented model (y_p) and the nonlinear UVA/Padova model (y) to a 1 U insulin bolus is calculated as:

$$\mathrm{RMSE} = \frac{\|y_p - y\|}{\sqrt{n}} \tag{3}$$

where $\|.\|$ indicates the 2-norm, and n is the number of samples. Because the simulator has a sampling time of 1 min, n has been defined as 2880 to capture the complete glucose variation from the operating point. It is worth remarking that steady-state glucose concentrations are achieved by only accommodating the insulin infusion rate. Consequently, the applied method to reach any initial state cannot influence subsequent glucose drops. Finally, the normalized RMSE (NRMSE) is computed as:

$$\mathrm{NRMSE} = \frac{\mathrm{RMSE}}{\mathrm{RMSE}_{\max}} \tag{4}$$

with $\mathrm{RMSE}_{\max}$ being the maximum RMSE obtained for all cases. The results for the complete CGM range of $[40, 400]$ mg/dl, and for a normal glucose target range of $[70, 180]$ mg/dl are shown in Table 1.

As presented in Colmegna et al. (2018), a complete comparison includes the computation of the ν-gap metric that considers the distance between two models according to their achievable closed-loop performance (Vinnicombe, 1993, 2001). However, that analysis is out of the scope of this work.

LQG synthesis

A CGM sensor usually provides glucose readings every 5 min. Because the AP control system operates in discrete-time, the continuous-time plant model $\mathcal{G}_j(s)$ is converted to the discrete-time plant model $\mathcal{G}_j(z)$ at this stage. To this end, model (2), without considering the 15-min delay, is discretized using a Zero Order Hold (ZOH) method with a sampling time $T_s = 5$ min. Let:

$$\bar{\mathcal{G}}_j(z) \equiv \left[\begin{array}{c|c} \bar{\mathbf{A}}_j & \bar{\mathbf{B}}_j \\ \hline \bar{\mathbf{C}}_j & 0 \end{array}\right] \tag{5}$$

be a third-order (minimal) realization of the resulting discrete-time model, where matrices $\bar{\mathbf{A}}_j \in \mathbb{R}^{3\times3}$, $\bar{\mathbf{B}}_j \in \mathbb{R}^{3\times1}$, and $\bar{\mathbf{C}}_j \in \mathbb{R}^{1\times3}$. Then, the discrete representation of (2) is obtained by adding the three-sample delay as follows:

$$\mathcal{G}_j(z) \equiv \left[\begin{array}{c|c} \mathbf{A}_j & \mathbf{B}_j \\ \hline \mathbf{C}_j & 0 \end{array}\right] \tag{6}$$

with

$$\mathbf{A}_j = \begin{bmatrix} \bar{\mathbf{A}}_j & \mathbf{0}_{3\times2} & \bar{\mathbf{B}}_j \\ \mathbf{0}_{1\times3} & \mathbf{0}_{1\times2} & 0 \\ \mathbf{0}_{2\times3} & \mathbf{I}_{2\times2} & \mathbf{0}_{2\times1} \end{bmatrix}, \tag{7}$$

$$\mathbf{B}_j = \begin{bmatrix} \mathbf{0}_{3\times1} & 1 & \mathbf{0}_{2\times1} \end{bmatrix}^T \quad \text{and} \quad \mathbf{C}_j = \begin{bmatrix} \bar{\mathbf{C}}_j & \mathbf{0}_{1\times3} \end{bmatrix},$$

where $\mathbf{0}_{i\times j}$ represents the zero matrix of order $i \times j$, and $I_{2\times2}$ represents the identity matrix of order 2. Finally, model $\mathcal{G}_j(z)$ is reduced to a third-order model defined as $\mathcal{G}_{r,j}(z)$ via the square root balance truncation algorithm (Safonov & Chiang, 1989). In Fig. 2, the result of this procedure is illustrated for adult #1 of the distribution version of the UVA/Padova simulator. In that figure, the frequency responses of $\mathcal{G}_1(s)$, $\mathcal{G}_1(z)$ and $\mathcal{G}_{r,1}(z)$ are depicted, showing that the three models agree well over the frequency range of interest $[0, 0.1]$ rad/min associated with the blood glucose control problem.

For a given T1DM adult patient #j, two LQG controllers $\mathcal{K}_{i,j}(z)$ with $i \in \mathcal{I} = \{1, 2\}$ are synthesized based on the following realization of $\mathcal{G}_{r,j}(z)$:

$$\begin{aligned} \mathbf{x}(k+1) &= \mathbf{A}_{r,j}\mathbf{x}(k) + \mathbf{B}_{r,j}u_\Delta(k) \\ y_\Delta(k) &= \mathbf{C}_{r,j}\mathbf{x}(k) \end{aligned} \tag{8}$$

with $u_\Delta(k) = u(k) - i_{b,j}$, and $y_\Delta(k) = y(k) - 120$ mg/dl, and $i_{b,j}$ is the patient-specific time-dependent basal input rate [pmol/min]. Then, a state-feedback control:

$$u_\Delta(k) = -\mathbf{K}_{i,j}\mathbf{x}(k) \tag{9}$$

that minimizes the following quadratic cost function:

$$J_i(u_\Delta, y_\Delta) = \sum_{k=0}^{\infty} \left(R_i u_\Delta^2 + Q y_\Delta^2 \right) \tag{10}$$

with $R_1 = 1$, $R_2 = 0.5$, and $Q = 5 \times 10^3$ is designed. Parameter R_2 is purposefully defined smaller than R_1 for $\mathcal{K}_{2,j}(z)$ to be more aggressive

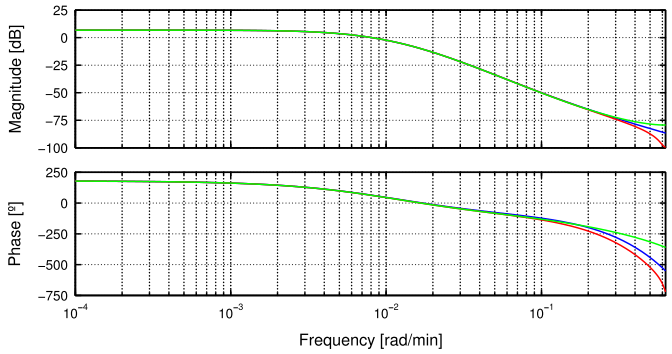

Fig. 2. Frequency responses of $\mathcal{G}_1(s)$ (blue line), $\mathcal{G}_1(z)$ (red line), and $\mathcal{G}_{r,1}(z)$ (green line). (For interpretation of the references to color in this figure legend, the reader is referred to the web version of this article.)

than $\mathcal{K}_{1,j}(z)$. In addition, states are estimated by a Kalman filter of the form:

$$\hat{\mathbf{x}}(k+1|k) = \mathbf{A}_{r,j}\hat{\mathbf{x}}(k|k-1) + \mathbf{B}_{r,j}u_{\Delta}(k) + \dots \\ \cdots + \mathbf{L}_{i,j}[y_{\Delta}(k) - \mathbf{C}_{r,j}\hat{\mathbf{x}}(k|k-1)] \tag{11}$$

where $\mathbf{L}_{i,j}$ is obtained assuming that process $w(k)$ and measurement $v(k)$ noises are uncorrelated white processes that satisfy

$$E[w(k)w(k)^T] = W, \quad E[v(k)v(k)^T] = V_i \tag{12}$$

with $W = V_1 = 3$, and $V_2 = 45 \times 10^{-4}$. Note that V_2 is intentionally smaller than V_1 in order to make $\mathcal{K}_{2,j}(z)$ be much faster than $\mathcal{K}_{1,j}(z)$.

Finally, since both LQG controllers have the structure of an observer with state-feedback, they have realizations $\{\mathbf{A}_{r,j} - \mathbf{L}_{i,j}\mathbf{C}_{r,j} - \mathbf{B}_{r,j}\mathbf{K}_{i,j}, \mathbf{L}_{i,j}, \mathbf{K}_{i,j}\}$ according to the previous design procedure.

Building the multicontroller

As mentioned above, two LQG controllers $\mathcal{K}_{i,j}$ with $i \in \mathcal{I}$ are synthesized for each T1DM adult #j. Here, a switched controller $\mathcal{C}_j(\sigma)$ that switches amongst both $\mathcal{K}_{i,j}$ is built with a convenient structure based on the Youla parameterization approach (Youla, Jabr, & Bongiorno, 1976). Multicontroller $\mathcal{C}_j(\sigma)$ is designed with three inputs: the switching signal σ, the quantized and saturated control signal $u_{C,qsat}$,[1] and the error signal e, and one output: the control signal u_C. The input $\sigma : [0,\infty) \to \mathcal{I}$ is piecewise constant. While σ remains constant and equal to some $i \in \mathcal{I}$, $\mathcal{C}_j(\sigma)$ is required to behave as an LTI system with transfer function $\mathcal{K}_{i,j}$, and in that case, u_C corresponds to u_{Δ}. The procedure to define $\mathcal{C}_j(\sigma)$ can be described as follows (see Hespanha and Morse (2002) for details).

First, according to Lemma 8 of Hespanha and Morse (2002), because the control-oriented model $\mathcal{G}_{r,j}$ is strictly proper and $\mathcal{K}_{1,j}$, which is also strictly proper, stabilizes $\mathcal{G}_{r,j}$, there exist matrices $\mathbf{A}_{E,j}$, $\mathbf{B}_{E,j}$, $\mathbf{C}_{E,j}$, $\mathbf{D}_{E,j}$, $\mathbf{F}_{E,j}$, and $\mathbf{G}_{E,j}$ (with appropriate dimensions) such that $\mathbf{A}_{E,j}$ is a stability matrix, and $\{\mathbf{A}_{E,j} + \mathbf{D}_{E,j}\mathbf{C}_{E,j}, \mathbf{B}_{E,j}, \mathbf{C}_{E,j}\}$ and $\{\mathbf{A}_{E,j} - \mathbf{B}_{E,j}\mathbf{F}_{E,j}, \mathbf{D}_{E,j} - \mathbf{B}_{E,j}\mathbf{G}_{E,j}, \mathbf{F}_{E,j}, \mathbf{G}_{E,j}\}$ are stabilizable and detectable realizations of $\mathcal{G}_{r,j}$ and $\mathcal{K}_{1,j}$, respectively. A way to define those matrices is stated in the proof of Lemma 8. Let $\{\mathbf{A}_{r,j}, \mathbf{B}_{r,j}, \mathbf{C}_{r,j}\}$ and $\{\mathbf{F}_j, \mathbf{G}_j, \mathbf{H}_j\}$ be minimal realizations of $\mathcal{G}_{r,j}$ and $\mathcal{K}_{1,j}$, respectively, and $\mathbf{X}_j$, $\mathbf{Y}_j$ matrices such that $\mathbf{A}_{r,j} + \mathbf{X}_j\mathbf{C}_{r,j}$ and $\mathbf{F}_j + \mathbf{Y}_j\mathbf{H}_j$ are asymptotically stable, then:

$$\mathbf{A}_{E,j} = \begin{bmatrix} \mathbf{A}_{r,j} + \mathbf{X}_j\mathbf{C}_{r,j} & \mathbf{0} \\ \mathbf{0} & \mathbf{F}_j + \mathbf{Y}_j\mathbf{H}_j \end{bmatrix}, \ \mathbf{B}_{E,j} = \begin{bmatrix} \mathbf{B}_{r,j} \\ -\mathbf{Y}_j \end{bmatrix}$$
$$\mathbf{C}_{E,j} = \begin{bmatrix} \mathbf{C}_{r,j} & \mathbf{0} \end{bmatrix}, \quad \mathbf{D}_{E,j} = \begin{bmatrix} -\mathbf{X}_j \\ -\mathbf{G}_j \end{bmatrix}$$
$$\mathbf{F}_{E,j} = \begin{bmatrix} \mathbf{0} & -\mathbf{H}_j \end{bmatrix}, \quad \mathbf{G}_{E,j} = \mathbf{0}. \tag{13}$$

[1] The quantized and saturated control signal $u_{C,qsat}$ is included as an input to $\mathcal{C}_j(\sigma)$ in order to consider the insulin pump constraints in the controller structure.

Next:

$$S_{i,j} = \left(Y_{C,j} + X_{C,j}\mathcal{K}_{i,j}\right)\left(X_{P,j} + Y_{P,j}\mathcal{K}_{i,j}\right)^{-1} \tag{14}$$

is defined as the Youla parameter with:

$$\begin{bmatrix} X_{C,j} & -Y_{C,j} \\ Y_{P,j} & X_{P,j} \end{bmatrix} = \begin{bmatrix} \mathbf{F}_{E,j} \\ \mathbf{C}_{E,j} \end{bmatrix}(s\mathbf{I} - \mathbf{A}_{r,j})^{-1}\begin{bmatrix} \mathbf{B}_{E,j} & -\mathbf{D}_{E,j} \end{bmatrix} + \dots \\ \cdots + \begin{bmatrix} \mathbf{I} & \mathbf{0} \\ \mathbf{0} & \mathbf{I} \end{bmatrix} \tag{15}$$

being a simultaneous coprime factorization of $K_{1,j}$ and $\mathcal{G}_{r,j}$. Note that if Eq. (14) is solved for $\mathcal{K}_{i,j}$, then:

$$\mathcal{K}_{i,j} = \left(X_{C,j} - S_{i,j}Y_{P,j}\right)^{-1}\left(Y_{C,j} + S_{i,j}X_{P,j}\right). \tag{16}$$

From Eq. (16), it is straightforward to see that if $K_{1,j}$ is selected as the central controller, i.e., $K_{1,j} = X_{C,j}^{-1}Y_{C,j}$, therefore, $S_{1,j} = 0$ by construction. In addition, the poles of $S_{2,j}$ must have magnitudes less than 1, because $\mathcal{K}_{2,j}$ stabilizes $\mathcal{G}_{r,j}$ (see Remark 10 in Appendix A of Hespanha and Morse (2002)). As a result, given a minimal stable realization $\{\mathbf{A}_{S,2,j}, \mathbf{B}_{S,2,j}, \mathbf{C}_{S,2,j}\}$ for $S_{2,j}$, the trivial realization $\{\mathbf{A}_{S,1,j}, \mathbf{B}_{S,1,j}, \mathbf{C}_{S,1,j}\} = \{\mathbf{A}_{S,2,j}, \mathbf{B}_{S,2,j}, \mathbf{0}\}$ can be picked for $S_{1,j}$. Thus, there exists a symmetric, positive definite matrix $\mathbf{Q}_j$, such that:

$$\mathbf{A}_{S,i,j}^T\mathbf{Q}_j\mathbf{A}_{S,i,j} - \mathbf{Q}_j < 0 \tag{17}$$

for $i \in \mathcal{I}$. This allows to select reset matrices as simply the identity. As stated in Lemma 1 of Hespanha and Morse (2002), the switched system that switches amongst both $S_{i,j}$ according to the value of the switching signal $\sigma : [0,\infty) \to \mathcal{I}$, i.e., $S_{\sigma,j}$, is exponentially stable, uniformly over $\mathcal{I}$.

Finally, the switched LQG controller $\mathcal{C}_j(\sigma)$ can be described by the following dynamical system:

$$\mathbf{x}_C(k+1) = \mathbf{A}_{C,j}\mathbf{x}_C(k) + \mathbf{B}_{C,j}\begin{bmatrix} u_{C,qsat}(k) \\ e(k) \end{bmatrix} \\ u_C(k) = \mathbf{C}_{C,\sigma,j}\mathbf{x}_C(k) \tag{18}$$

with

$$\mathbf{A}_{C,j} = \begin{bmatrix} \mathbf{A}_{E,j} & \mathbf{0} \\ \mathbf{B}_{S,2,j}\mathbf{C}_{E,j} & \mathbf{A}_{S,2,j} \end{bmatrix}, \\ \mathbf{B}_{C,j} = \begin{bmatrix} \mathbf{B}_{E,j} & -\mathbf{D}_{E,j} \\ \mathbf{0} & \mathbf{B}_{S,2,j} \end{bmatrix}, \quad \mathbf{C}_{C,\sigma,j} = \begin{bmatrix} -\mathbf{F}_{E,j} & \mathbf{C}_{S,\sigma,j} \end{bmatrix}. \tag{19}$$

According to Theorem 5 of Hespanha and Morse (2002), the feedback connection between $\mathcal{C}_j(\sigma)$ and the process model $\mathcal{G}_{r,j}$ is exponentially stable, uniformly over $\mathcal{I}$. Although this could be considered a secondary result in this particular application, note that the resulting controller structure allows arbitrary switching amongst both LQG controllers $\mathcal{K}_{i,j}$, switching solely matrix $\mathbf{C}_{S,i,j}$. In addition, because reset matrices are simple the identity, the controller's state is not reset at switching times. As a consequence, the state of the switched controller is always consistent with the state of the "plant".

2.2. SAFE layer for IOB constraints

In this section the SAFE method presented in Revert et al. (2013) is reformulated in a simplified version and added to the switched LQG control scheme. This mechanism is based on sliding mode conditioning concepts (Garelli, Mantz, & De Battista, 2011) as a way to reduce hypoglycemic events, which could be induced by the main closed-loop controller. To this end, it adapts the controller's gain to avoid (or to try to avoid in case of external boluses) violating a patient-specific constraint on the IOB denoted by $\overline{\text{IOB}}_j(t)$. In this way, it provides a safety layer that can be adjusted according to medical criteria, and improves robustness against over-estimated insulin doses.

In Fig. 3 the subsystems composing the SAFE block of the ARG algorithm are depicted. The switching logic $w(t)$ is:

$$w(t) = \begin{cases} 1 & \text{if } \sigma_{\text{SM}}(t) > 0 \\ 0 & \text{otherwise} \end{cases} \tag{20}$$

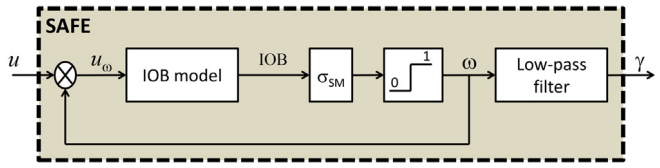

Fig. 3. Block diagram associated with the SAFE mechanism.

with the sliding function $\sigma_{\text{SM}}(t)$ for this version of SAFE being the trivial function:

$$\sigma_{\text{SM}}(t) = \overline{\text{IOB}}_j(t) - \text{IOB}(t). \tag{21}$$

In this work, piecewise constant $\overline{\text{IOB}}_j(t)$ profiles are considered as discussed below.

Because the IOB cannot be measured in real-time, it must be estimated. To this end, the dynamical model presented in Willinska et al. (2005) that can be personalized based solely on *a priori* clinical information is considered:

$$\begin{aligned}\dot{I}_{sc1}(t) &= -K_{\text{DIA}} I_{sc1}(t) + u_w(t) \\ \dot{I}_{sc2}(t) &= K_{\text{DIA}} \left[I_{sc1}(t) - I_{sc2}(t)\right] \\ \text{IOB}(t) &= I_{sc1}(t) + I_{sc2}(t)\end{aligned} \tag{22}$$

where I_{sc1} and I_{sc2} are, respectively, the amount of nonmonomeric and monomeric insulin in the subcutaneous space, u_w is the exogenous insulin infusion rate in [pmol/min/kg], and K_{DIA} [min^{-1}] is a constant that has to be tuned for each patient so as to replicate its corresponding Duration of Insulin Action (DIA). A method to calculate the patient's DIA is detailed in Walsh and Roberts (2006). Here, a 5 h DIA is selected, hence K_{DIA} is set to 16.3×10^{-3} [min^{-1}] according to León-Vargas, Garelli, De Battista, and Vehi (2015). A unique K_{DIA} is defined for all cases in order to reduce the number of parameters needed to initialize the control strategy. In any case, if it results unsuitable for a particular patient because of repeated hypo- or hyperglycemic events, it can be personalized, e.g., by a run-to-run method. It is worth mentioning that any other proposals to estimate the IOB could also be employed (Bequette, 2009; Ellingsen et al., 2009; Patek et al., 2012), including those based on CGM measurements (de Pereda et al., 2016).

When the given $\overline{\text{IOB}}_j(t)$ constraint is reached, a transient sliding regime is established on the sliding surface $\sigma_{\text{SM}}(t) = 0$. During this mode, according to (20), $w(t)$ switches at very fast frequency between 0 and 1 in order to fulfill the constraint and force system (22) to remain in the invariance set

$$\Sigma = \{\mathbf{x}(t) \mid \sigma_{\text{SM}}(t) \geq 0\} \tag{23}$$

where $\mathbf{x}(t) \in \mathbb{R}^2$ is the state of system (22). In order to avoid the chattering phenomena in the pump command signal, a low-pass first-order filter is implemented to smooth out the switching signal $w(t)$, yielding $\gamma(t)$. Note that this filter could be simply the average of $w(t)$ in the interval between insulin infusion times.

Remark. Re-writing model (22) as:

$$\begin{aligned}\dot{\mathbf{x}}(t) &= f(\mathbf{x}) + g(\mathbf{x})u_w(t) = \cdots \\ \cdots &= \begin{bmatrix} -K_{\text{DIA}} I_{sc1}(t) \\ K_{\text{DIA}} \left[I_{sc1}(t) - I_{sc2}(t)\right] \end{bmatrix} + \begin{bmatrix} 1 \\ 0 \end{bmatrix} u_w(t)\end{aligned} \tag{24}$$

where $f(\mathbf{x}) : \mathbb{R}^2 \to \mathbb{R}^2$ and $g(\mathbf{x}) : \mathbb{R}^1 \to \mathbb{R}^2$ are vector fields, the necessary condition that must be fulfilled for the sliding mode to exist is the transversality condition, that is $L_g \sigma_{\text{SM}}(t) = \frac{\partial \sigma_{\text{SM}}(t)}{\partial \mathbf{x}}(t) g(\mathbf{x}) \neq 0$. Here,

$$L_g \sigma_{\text{SM}}(t) = \begin{bmatrix} -1 & -1 \end{bmatrix} \begin{bmatrix} 1 \\ 0 \end{bmatrix} = -1 \neq 0, \tag{25}$$

i.e., the transversality condition always holds.

Clearly, the SAFE mechanism is implemented as a discrete version of (22), as follows:

$$\begin{aligned}\mathbf{x}(k+1) &= \begin{bmatrix} 1 - K_{\text{DIA}} T_r & 0 \\ K_{\text{DIA}} T_r & 1 - K_{\text{DIA}} T_r \end{bmatrix} \mathbf{x}(k) + \begin{bmatrix} 1 \\ 0 \end{bmatrix} u_w(k) \\ \text{IOB}(k) &= \begin{bmatrix} 1 & 1 \end{bmatrix} \mathbf{x}(k)\end{aligned} \tag{26}$$

with $T_r = 0.1$ min being the selected sampling time. Note that T_r is much lower than $T_s = 5$ min. The main reason for this is that the whole SAFE algorithm is completely software based, and thus its switching frequency is physically limited only by the microprocessor speed.

IOB constraint definition

The standard IOB limit $\overline{\text{IOB}}_j(t)$ for meals is defined as:

$$\overline{\text{IOB}}_j(t) = \overline{\text{IOB}}_{\text{m},j}(t) = \text{IOB}_{\text{ss},j}(t) + 55 \text{ gCHO/CR}_j(t) \tag{27}$$

where $\text{IOB}_{\text{ss},j}(t)$ is the steady-state response of model (26), considering the patient-specific current basal input rate $i_{b,j}(t)$, and 55 $\text{gCHO/CR}_j(t)$ is the insulin bolus related to a 55 g of carbohydrates (gCHO) using the current patient's Carbohydrate Ratio (CR) in [g/U]. Naturally, this definition is a starting-point. Then, $\overline{\text{IOB}}_j(t)$ should be tuned in terms of postprandial hypo- or hyperglycemia frequency.

It is worth remarking that $\overline{\text{IOB}}_j(t)$ implies simply a limit, and not the exact amount of insulin to be injected. For example, the constraint $\overline{\text{IOB}}_j(t)$ is likely to be high enough to not be violated by the switched LQG controller when the patient ingests a small meal, but that situation does not necessarily imply an excessive amount of insulin to be commanded by the controller. On the other hand, when the patient ingests a large meal, it does not necessarily involve postprandial hyperglycemia, because the controller will react according to the CGM signal, and in such a case the sliding regime will be established for a longer duration. This means that $\overline{\text{IOB}}_j(t)$ does not only guarantee safety for a 55 gCHO meal, but for a meal size interval also. However, in order to add another degree of freedom to the controller structure, an $\overline{\text{IOB}}_j(t)$ that depends on a meal size classification could be defined as follows:

- Small meals < 35 gCHO. $\overline{\text{IOB}}_{\text{s},j}(t) = \text{IOB}_{\text{ss},j}(t) + 40$ $\text{gCHO/CR}_j(t)$.
- Medium meals [35, 65) gCHO. $\overline{\text{IOB}}_{\text{m},j}(t) = \text{IOB}_{\text{ss},j}(t) + 55$ gCHO $/\text{CR}_j(t)$.
- Large meals ≥ 65 gCHO. $\overline{\text{IOB}}_{\text{l},j}(t) = \text{IOB}_{\text{ss},j}(t) + 70$ $\text{gCHO/CR}_j(t)$.

The use of a meal size classification can also be found in El-Khatib et al. (2017), Gingras, Haidar et al. (2016) and Gingras, Rabasa-Lhoret et al. (2016) where it is used to apply premeal insulin boluses. Both approaches, with and without meal size classification, will be simulated later. When the system is not coping with a meal-related situation, the IOB limit is set by default to $\overline{\text{IOB}}_{\text{s},j}(t)$ so as to let the controller command slight changes on the basal infusion rate.

2.3. Multicontroller switching mechanism

As mentioned before, $\mathcal{K}_{2,j}$ is applied only at meal times to generate an insulin spike akin to the standard open-loop basal-bolus treatment. The problem at this point is how a meal-related situation is detected and, consequently, how the IOB limit is changed according to that. There are two strategies: manual announcement, which is the strategy selected in this work, and automatic detection. Next, both will be discussed.

Meal time announcement

In this simple approach the patient has to announce the meal time, for example by simply pushing a button. The use of qualitative meal announcement was discussed in Steil et al. (2006) as a way to adjust the aggressiveness of the control algorithm in certain situations, in this case after a meal intake. If a meal size classification scheme is followed, then the user has to select also the meal size (small, medium or large). This signal triggers the ARG algorithm to a *listening* mode that will remain active for 90 min at most. In the algorithm, the *listening* mode state

is represented by a boolean variable ℓ that is zero by default and is set to unity when the *listening* mode is active. During this mode, the aggressive LQG controller is selected when rising glucose values are inferred from the CGM trend. In that case, $\overline{\text{IOB}}_j(t)$ is changed from $\overline{\text{IOB}}_{s,j}(t)$ to the corresponding IOB limit. Its value depends whether or not a meal size classification is being used. Then, the aggressive controller will command the insulin infusion during an hour. After that the conservative controller will automatically take over the insulin delivery, and 30 min later, the $\overline{\text{IOB}}_j(t)$ will be set to $\overline{\text{IOB}}_{s,j}(t)$ again.

Automatic meal detection

The ARG algorithm is independent of the way on which meals are detected. Therefore, any pre-existing meal detection algorithm (Colmegna et al., 2016b; Dassau, Bequette, Buckingham, & Doyle III, 2008; Harvey, Dassau, Zisser, Seborg, & Doyle III, 2008; Hughes, Patek, Breton, & Kovatchev, 2011; Samadi et al., 2017; Turksoy et al., 2016) can be employed for the generation of the switching signal σ that commands which LQG controller is selected.

In general, if the detection depends on the CGM signal, some unrealistic hyperglycemic conditions may be detected because of the high measurement noise. Consequently, there is a compromise between a fast response and CGM noise immunity. For that reason, and due to the fact that the ARG algorithm was intended to be applied in a clinical trial for the first time, an automatic detection is not considered in this work.

2.4. Auxiliary modules

In order to minimize the risks of hypo- and hyperglycemia, two auxiliary modules, which are discussed below, have been added to the ARG algorithm to make it more robust against the time-varying nature and high uncertainty of the insulin-glucose dynamics.

Hypoglycemia-related module (Hypo-RM)

Here, an algorithm to lower the IOB limit when low glucose values are detected or predicted is defined as follows.

1: At every sampling time:
2: The glucose measured by the CGM sensor (g) in mg/dl is received, and a linear extrapolation strategy is used to estimate the glucose rate of change ($\hat{g}_{30}$) in mg/dl/min. Besides, the future glucose concentration is predicted with a forecasting horizon of 15 min ($\hat{g}_{15}$), considering the last six glucose measurements, i.e., the CGM samples received during the last 30 min.
3: The IOB limit is set according to previous sections.
4: **if** $g < 60$ **then**
5: $\quad\overline{\text{IOB}}_j(t) = 0$
6: **else if** $g < 70$ **then**
7: $\quad\overline{\text{IOB}}_j(t) = 0.5\text{IOB}_{\text{ss},j}(t)$
8: **else if** $i = 1$ **and** $\ell = 0$ **then**
9: $\quad$**if** $\hat{g}_{30} < -0.5$ **or** $[\hat{g}_{30} < 0.5$ **and** $\text{IOB}(t) \geq \text{IOB}_{\text{ss},j}(t)]$ **then**
10: $\quad\quad$**if** $\hat{g}_{15} < 70$ **then**
11: $\quad\quad\quad\overline{\text{IOB}}_j(t) = 0.5\text{IOB}_{\text{ss},j}(t)$
12: $\quad\quad$**else if** $\hat{g}_{15} < 100$ **then**
13: $\quad\quad\quad\overline{\text{IOB}}_j(t) = 0.75\text{IOB}_{\text{ss},j}(t)$
14: $\quad\quad$**else if** $\hat{g}_{15} < 120$ **then**
15: $\quad\quad\quad\overline{\text{IOB}}_j(t) = \text{IOB}_{\text{ss},j}(t)$
16: $\quad\quad$**end if**
17: $\quad$**end if**
18: **end if**

In this way, the Hypo-RM module has the following levels of action:

- **Level A**: $\overline{\text{IOB}}(t) = 0$.
- **Level B**: $\overline{\text{IOB}}(t) = 0.5\text{IOB}_{\text{ss}}(t)$.
- **Level C**: $\overline{\text{IOB}}(t) = 0.75\text{IOB}_{\text{ss}}(t)$.
- **Level D**: $\overline{\text{IOB}}(t) = \text{IOB}_{\text{ss}}(t)$.

In addition, note that the code below Line 8 is executed only if the controller is in conservative mode ($i = 1$) and in non-*listening* mode ($\ell = 0$).

Hyperglycemia-related module (Hyper-RM)

This module generates a Correction Bolus (CB) in [U] based on the patient's Correction Factor (CF) in [U/mg/dl] when a persistent hyperglycemic excursion cannot be mitigated by the conservative mode of the ARG algorithm.

1: At every sampling time:
2: A boolean variable HYPOFLAG is set to unity if the Hypo-RM was activated, and to zero otherwise.
3: The glucose rate of change ($\hat{g}_{30}$) and the future glucose concentration ($\hat{g}_{15}$) determined in the Hypo-RM are considered here, together with the glucose rate of change estimated from the last three CGM samples ($\hat{g}_{15}$).
4: The mean value of the last six CGM samples ($\bar{g}_{30}$) is calculated.
5: A boolean variable G160FLAG, which is zero by default, is set to unity if the last six CGM samples are higher than 160 mg/dl.
6: Timers CCBOLUS and CAGGCON that count the minutes elapsed from the last CB and from the last aggressive-conservative commutation are updated.
7: **if** $i = 1$ **and** $\ell = 0$ **then**
8: $\quad$**if** HYPOFLAG $= 0$ **and** CCBOLUS ≥ 120 **and** CAGGCON ≥ 180 **then**
9: $\quad\quad$**if** (G160FLAG $= 1$ **and** $\hat{g}_{30} \geq 0$ **and** $\hat{g}_{15} \geq -0.5$) **or** $\bar{g}_{30} > 200$ **then**
10: $\quad\quad\quad\text{CB} = 0.8[\min(\bar{g}_{30}, \hat{g}_{15})\text{-}120]/\text{CF}$
11: $\quad\quad$**end if**
12: $\quad$**end if**
13: **end if**

Note that according to the conditions that have to be fulfilled for the generation of a CB, this module is likely to be activated only during fasting periods of persistent hyperglycemia. The minimum between $\bar{g}_{30}$ and $\hat{g}_{15}$, and the 0.8 factor are considered to be conservative, because the measurement noise could lead to overestimate the value of the CB. In addition, for safety, the CB is not directly infused to the patient, but it is added to the insulin bolus proposed by the ARG algorithm to avoid violating the IOB limit by means of the SAFE layer.

3. Results

In this section the closed-loop results from the simulation and experimental studies with the ARG control structure are presented.

3.1. In silico studies

Before the clinical trial, the ARG algorithm was rigorously tested *in silico*. Here, some results are presented considering the following:

- the complete *in silico* adult cohort of the 300 subject FDA-accepted UVA/Padova simulator, a CGM as sensor, and a CSII pump;
- the fasting state of each *in silico* subject at the start of the simulation;
- a constant reference of 120 mg/dl;
- no carbohydrate treatments;
- no meal size classification unless stated otherwise; and
- the 5 h time interval following the start of meal as a Postprandial Period (PP) defined for performance analysis.

In order to illustrate how the ARG algorithm works, the closed-loop response for adult #1 to a meal of 50 gCHO ingested five hours after the start of the simulation is depicted in Fig. 4. As shown in that figure, when $\mathcal{K}_{2,j}$ is selected ($\sigma = 2$), insulin delivery experiences spikes, reducing postprandial glucose levels. Immediately after the IOB reaches its limit, a fast switching sequence occurs on the constraint

Table 2
In silico closed-loop results with the ARG algorithm. The overall (O), and the PP time interval defined previously are analyzed separately.

		50 gCHO meal			25 gCHO meal			75 gCHO meal			Two 50 gCHO meals		
		Mean	Median	IQR	Mean	Median	IQR	Mean	Median	IQR	Mean	Median	IQR
Blood Glucose [mg/dl]	O	134	133	[128, 137]	127	126	[121, 131]	143	142	[136, 148]	140	139	[133, 145]
	PP	160	159	[150, 167]	135	133	[126, 141]	188	186	[175, 196]	155	155	[146, 163]
% time in [70, 250] mg/dl	O	99.6	100	[100, 100]	99.7	100	[100, 100]	96.7	100	[94.8, 100]	99.4	100	[100, 100]
	PP	99.0	100	[100, 100]	99.4	100	[100, 100]	89.7	100	[83.3, 100]	99.2	100	[100, 100]
% time in [70, 180] mg/dl	O	89.8	90.9	[88.1, 92.2]	98.7	100	[100, 100]	83.0	83.8	[80.6, 86.8]	84.4	85.5	[80.9, 88.5]
	PP	67.7	71.0	[62.0, 75.0]	96.3	100	[100, 100]	46.4	48.0	[38.0, 57.8]	72.2	74.0	[65.7, 79.4]
% time < 70 mg/dl	O	0.1	0.0	[0.0, 0.0]	0.3	0.0	[0.0, 0.0]	0.1	0.0	[0.0, 0.0]	0.3	0.0	[0.0, 0.0]
	PP	0.1	0.0	[0.0, 0.0]	0.6	0.0	[0.0, 0.0]	0.0	0.0	[0.0, 0.0]	0.2	0.0	[0.0, 0.0]
% time < 50 mg/dl	O	0.0	0.0	[0.0, 0.0]	0.0	0.0	[0.0, 0.0]	0.0	0.0	[0.0, 0.0]	0.0	0.0	[0.0, 0.0]
	PP	0.0	0.0	[0.0, 0.0]	0.1	0.0	[0.0, 0.0]	0.0	0.0	[0.0, 0.0]	0.0	0.0	[0.0, 0.0]
LBGI		0.1	0.0	[0.0, 0.0]	0.1	0.0	[0.0, 0.1]	0.0	0.0	[0.0, 0.1]	0.1	0.0	[0.0, 0.1]
HBGI		2.0	1.8	[1.5, 2.3]	0.9	0.8	[0.6, 1.2]	3.6	3.3	[2.7, 4.0]	2.9	2.6	[2.1, 3.4]
Amount of insulin injected [U]		21.0	20.0	[17.0, 24.0]	20.0	19.0	[17.0, 24.0]	22.0	21.0	[19.0, 25.0]	27.0	25.0	[23.0, 31.0]

IQR, interquartile range.

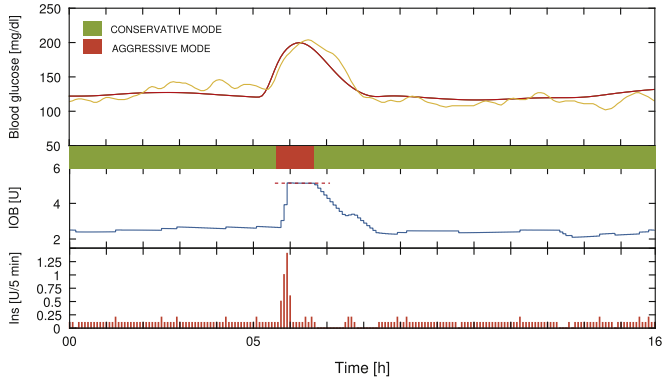

Fig. 4. Closed-loop response for adult #1 of the UVA/Padova simulator to a 50 gCHO meal. **Above:** Blood glucose concentration (red), and CGM signal (orange). **Middle**: IOB estimation. The red dashed line indicates the IOB limit $\overline{\text{IOB}}_{\text{m},1}$. **Below:** Insulin infusion. (For interpretation of the references to color in this figure legend, the reader is referred to the web version of this article.)

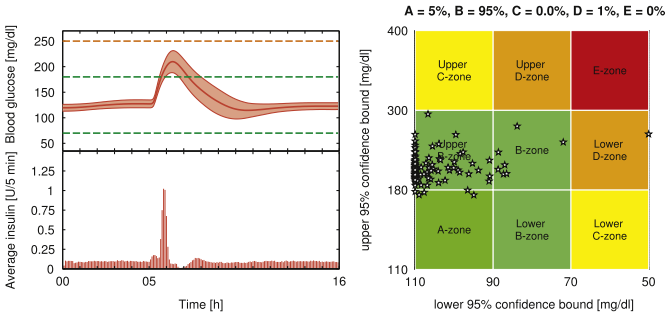

Fig. 5. Average closed-loop response for all the *in silico* adults of the 300 subject UVA/Padova simulator (left) and the CVGA plot (right) to a 50 gCHO meal. **Upper-left:** The thick lines are the mean blood glucose values, and the boundaries of the filled areas are the mean ±1 STD values. Dashed lines (green and orange) represent the limits of the 70–180 mg/dl and 70–250 mg/dl ranges. **Bottom-left:** Average insulin infusion. (For interpretation of the references to color in this figure legend, the reader is referred to the web version of this article.)

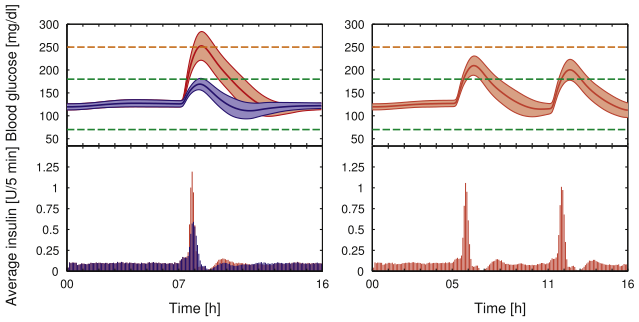

Fig. 6. Average closed-loop responses for all the *in silico* adults of the 300 subject UVA/Padova simulator to different sized meals. **Left:** 25 gCHO meal (blue) and 75 gCHO meal (red). **Right:** Two 50 gCHO meals. **Above:** The thick lines are the mean blood glucose values, and the boundaries of the filled areas are the mean ±1 STD values. Dashed lines (green and orange) represent the limits of the 70–180 mg/dl and 70–250 mg/dl ranges. **Below:** Average insulin infusions. (For interpretation of the references to color in this figure legend, the reader is referred to the web version of this article.)

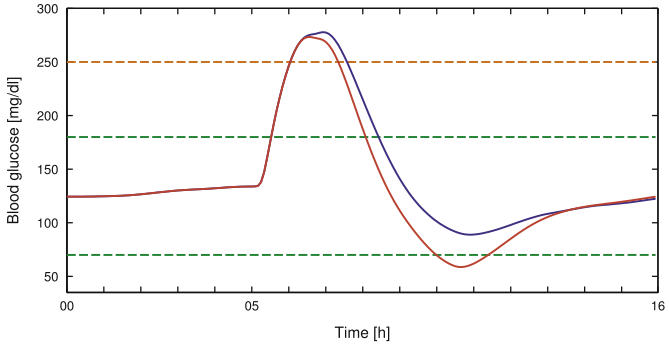

Fig. 7. Closed-loop response for adult #90 to a 50 gCHO meal with the standard IOB limit $\overline{\text{IOB}}_{\text{m},90}$ (red curve) and with a lower IOB limit: $0.7\overline{\text{IOB}}_{\text{m},90}$ (blue curve) for meals. Dashed lines (green and orange) represent the limits of the 70–180 mg/dl and 70–250 mg/dl ranges. (For interpretation of the references to color in this figure legend, the reader is referred to the web version of this article.)

$\sigma_{\text{SM}}(t) = \overline{\text{IOB}}_1(t) - \text{IOB}(t) = 0$, establishing a transient sliding regime. Finally, the filtered signal γ is used to modulate the control signal proposed by the switched LQG controller in order to command the CSII pump.

In Fig. 5, the Control Variability Grid Analysis (CVGA) plot (Magni et al., 2008) and the average time response to a 50 gCHO meal ingested five hours after the start of the simulation are presented. As shown in that figure, insulin spikes occur after the meal time is announced, and the aggressive LQG controller is selected. However, because of the time delay associated with the CGM technology, the increase in the glucose level due to the meal ingestion cannot be inferred immediately from the CGM signal when the *listening* mode is active. Consequently, the insulin

spikes needed to mitigate the glucose increase during the postprandial period have a delay of a few minutes. Thus, glucose peaks after meals are difficult to prevent (Atlas, Nimri, Miller, Grunberg, & Phillip, 2010; Reddy et al., 2015; Weinzimer et al., 2008), and most CVGA plots are in the upper B-zone. Average results for the overall (O) and the PP time intervals are presented in Table 2, showing a safe hypo- and hyperglycemic control. This is reflected, for example, in the values of Low Blood Glucose Index (LBGI) and High Blood Glucose Index (HBGI), which indicate a minimal risk of hypoglycemia (LBGI$\leq$ 1.1) and a low risk of hyperglycemia (HBGI$\leq$4.5) (Clarke & Kovatchev, 2009).

In order to analyze the closed-loop performance with differently sized meals, the average time responses to a 25 gCHO, 75 gCHO and two 50 gCHO meals are illustrated in Fig. 6, and the results are included in Table 2. In the first two cases, the meal time is seven hours after the simulation starts. In the last case, the first 50 gCHO meal is ingested five hours after the simulation starts, whereas the other 50 gCHO meal is ingested six hours later. Although the ARG algorithm provides safe blood glucose control in these cases as well, its performance could be improved if a meal size classification approach is followed. For example, when an IOB limit for small meals (<35 gCHO) is considered at meal time in the simulations with a 25 gCHO meal, the percentage of time in the range [70, 180] mg/dl is still 96.3% in average during the PP time interval, but the mean percentage of time below 70 mg/dl is reduced from 0.6% to 0.2%. On the other hand, when an IOB limit for large meals ($\geq$65 gCHO) is applied at meal time in the simulations with a 75 gCHO meal, the percentage of time in the range [70, 180] mg/dl is increased from 46.4% to 52.3% in average during the PP time interval, while the mean percentage of time below 70 mg/dl scarcely increased from 0.0% to 0.2%.

Finally, note that according to the CVGA plot presented in Fig. 5, one of the adults (adult #90) is in the Lower D-zone. Although the *in silico* database should not be evaluated as individuals, but as a whole population (Visentin, Dalla Man, Kovatchev, & Cobelli, 2014), this situation allows us to illustrate that the IOB limit can be tuned based on the postprandial behavior as stated before. In this case, if a new lower IOB limit is defined for adult #90, then postprandial hypoglycemia is avoided as depicted in Fig. 7.

3.2. Clinical trial

The first AP clinical trials in Latin America were divided in two stages. First, the UVA algorithm (Patek et al., 2012) was tested following a hybrid closed-loop strategy in November 2016 (Sánchez-Peña et al., 2017). Then, the ARG algorithm was validated during the second clinical stage in June 2017 without premeal insulin boluses. In both stages:

- the control algorithm was migrated into the DiAs platform;
- five (two male, three female) T1DM adult patients were considered;
- the inpatient studies were performed at the Hospital Italiano de Buenos Aires during 36 h;
- Roche's Accu-Check Combo® insulin pumps and Dexcom G4 Share® sensors were used; and
- 15 g of rescue carbohydrates were given when patients' blood glucose levels dropped below 70 mg/dl.

Here, a summary of the results obtained in the second clinical stage is presented to show the effectiveness of the proposed control strategy in regulating the glucose level in T1DM patients (a complete analysis of the results is an ongoing work in collaboration with the medical staff).

The five patients in the second clinical stage had an average age of 43 $\pm$ 6 years, a mean TDI of 38 $\pm$ 14 U, a mean HbA1c of 7.4 $\pm$ 0.7%, a mean weight of 65.3 $\pm$ 15.8 kg, and an average diabetes duration of 19 $\pm$ 5 years. The closed-loop study started on June 23 at 19:00 h and ended on June 25 at 07:00 h, involving two dinners, one breakfast, one lunch and one afternoon snack. Before each meal, the patients had to announce if the meal was small, medium or large by pushing a button through the DiAs system, which triggered the ARG algorithm to the *listening* mode. The meal size classification defined previously was adopted at this stage in order to minimize the IOB limit uncertainty, as it was the first time that this control strategy was going to be clinically tested.

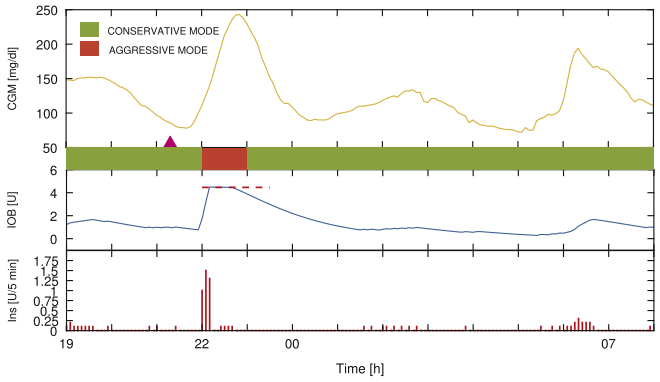

Fig. 8. Clinical closed-loop response for patient #54112 to a 55 gCHO meal. **Above:** CGM signal. The upward-pointing triangle indicates the meal time announcement. **Middle**: IOB estimation. The red dashed line indicates the IOB limit. **Below:** Insulin infusion. (For interpretation of the references to color in this figure legend, the reader is referred to the web version of this article.)

The closed-loop response for one of the patients (patient #54112) after a 55 gCHO meal (pasta + chicken breast + fruit) is illustrated in Fig. 8. It is noteworthy the similarity between this figure and Fig. 4. Although nearly at 06:00 h the glucose level increased rapidly, the ARG algorithm could mitigate that excursion without using the Hyper-RM module.

In Table 3 the average clinical results are presented, considering that:

- CGM readings during the first night and the following morning for one of the patients (patient #54115) were discarded due to an occlusion within the insulin pump during the trial.
- A mean number of 2 rescue doses of carbohydrates *per* patient was given. It is worth remarking that roughly the 50% of the carbohydrate treatments were given after the lunch. This is because the IOB limit for each patient was intentionally significantly increased before that meal to test the controller's aggressiveness.

The objective of this clinical study was not to compare the proposed closed-loop strategy with the standard open-loop basal-bolus treatment, because not all conditions were identical in both cases. Nevertheless, open-loop results that were obtained before carrying out the closed-loop test are also included in order to illustrate how the glucose control is improved with the ARG algorithm. Both the open- and closed-loop results consider the same hours during the day. Furthermore, because a better comparison is obtained during the night (N) when the patient is resting (from 23:00 h to 07:00 h), two nights (N_1 and N_2) are also analyzed separately in Table 3. Finally, the results from the last 15 h of the clinical trial are also presented. As shown in that table, there is an improvement in the control performance during that period of time where the initial transient is not included.

In Bequette (2012), the *dawn phenomena* is mentioned as a physiological event at roughly 04:00 h that causes the blood glucose concentration to rise, because of a reduction in patient's insulin sensitivity. In order to show the performance of the control algorithm in regulating the glucose level, in Fig. 9, it is illustrated how this phenomenon was mitigated in closed-loop for one of the patients (patient #54116).

Finally, concerning how often the safety mechanisms presented in Section 2.4 were activated during this trial, it is found that the number of times the Hyper-RM was activated *per* patient has median 1 and IQR [0, 2]. On the other hand, the Hypo-RM module was activated as follows:

- **Level A**: Median 1.7% of time and IQR: [1.1, 4.4]%.

Table 3
Average clinical results in open-loop (OL) and in closed-loop (CL). The 36 h and the 15 h periods, and the nights (N_1 and N_2) are analyzed separately. Statistically significant at $p < 0.05$.

36 h	OL			CL			*p*-value
	Mean	Median	IQR	Mean	Median	IQR	
Glucose [mg/dl]	153	157	[143, 165]	138	138	[127, 151]	0.121
% time in [70, 250] mg/dl	82.9	83.1	[77.0, 93.0]	88.6	88.2	[84.4, 93.2]	0.315
% time in [70, 180] mg/dl	59.1	55.5	[52.5, 62.9]	74.7	75.0	[69.7, 78.3]	0.036
% time < 70 mg/dl	7.6	6.3	[4.5, 11.1]	5.8	6.3	[3.1, 8.8]	0.290
% time < 50 mg/dl	1.7	1.4	[0.9, 2.8]	0.8	0.7	[0.0, 1.2]	0.189
LBGI[a]	2.8	2.5	[2.2, 3.3]	2.3	2.1	[1.8, 2.9]	0.215
HBGI	7.2	7.7	[5.6, 9.3]	4.9	4.3	[3.9, 5.9]	0.182
Amount of injected insulin [U][b]	63.7	57.7	[43.4, 84.0]	50.7	45.2	[36.6, 64.9]	0.049
15 h							
Glucose [mg/dl]	156	157	[145, 177]	129	128	[112, 148]	0.057
% time in [70, 250] mg/dl	73.5	83.3	[54.2, 88.8]	94.7	92.8	[90.7, 100]	0.083
% time in [70, 180] mg/dl	49.8	42.2	[39.3, 55.6]	82.6	85.0	[72.9, 91.5]	0.014
% time < 70 mg/dl	13.6	10.6	[8.6, 20.8]	4.1	1.1	[0.0, 9.3]	0.049
% time < 50 mg/dl	5.4	3.9	[2.5, 8.1]	0.2	0.0	[0.0, 0.3]	0.083
LBGI[a]	4.2	4.0	[2.9, 5.2]	1.8	1.6	[1.1, 2.8]	0.038
HBGI	8.7	9.4	[6.5, 11.0]	2.8	2.1	[1.2, 5.0]	0.047
Amount of injected insulin [U][b]	23.5	21.1	[15.7, 31.4]	18.4	16.0	[13.1, 23.7]	0.130
N_1							
Glucose [mg/dl]	196	198	[169, 222]	155	145	[125, 185]	0.336
% time in [70, 250] mg/dl	66.8	69.8	[48.1, 85.4]	84.4	87.5	[69.3, 99.5]	0.176
% time in [70, 180] mg/dl	26.4	22.0	[16.1, 36.6]	71.1	72.4	[56.3, 85.9]	0.072
% time < 70 mg/dl	12.0	12.6	[6.3, 17.8]	1.0	0.0	[0.0, 2.1]	0.105
% time < 50 mg/dl	3.4	2.1	[0.0, 6.8]	0.0	0.0	[0.0, 0.0]	0.226
LBGI[a]	3.1	3.7	[1.4, 4.8]	1.6	1.8	[1.2, 2.1]	0.337
HBGI	14.8	13.0	[10.0, 19.5]	8.1	6.2	[2.7, 13.6]	0.347
Amount of injected insulin [U][b]	8.5	9.0	[5.7, 11.4]	5.9	3.5	[2.9, 9.0]	0.261
N_2							
Glucose [mg/dl]	169	183	[137, 196]	125	118	[106, 141]	0.033
% time in [70, 250] mg/dl	78.1	94.9	[55.7, 100]	95.0	100	[91.1, 100]	0.341
% time in [70, 180] mg/dl	50.3	44.8	[35.9, 70.7]	87.7	82.3	[81.0, 96.1]	0.035
% time < 70 mg/dl	3.6	0.0	[0.0, 5.8]	5.0	0.0	[0.0, 8.9]	0.821
% time < 50 mg/dl	0.0	0.0	[0.0, 0.0]	0.0	0.0	[0.0, 0.0]	–
LBGI[a]	2.0	1.9	[1.0, 2.8]	1.5	1.1	[0.4, 2.6]	0.471
HBGI	9.8	10.6	[4.4, 14.3]	1.9	1.4	[0.1, 3.3]	0.031
Amount of injected insulin [U][b]	8.2	9.0	[5.6, 10.8]	5.4	5.2	[3.3, 7.5]	0.069

[a] Modified according to Fabris, Patek, and Breton (2016).
[b] Patient with pump occlusion during the trial has been excluded from this analysis.

- **Level B**: Median 6.5% of time and IQR: [5.5, 7.9]%.
- **Level C**: Median 7.0% of time and IQR: [6.2, 11.4]%.
- **Level D**: Median 5.0% of time and IQR: [4.5, 9.8]%.

It is worth remarking that the activation of the Hypo-RM does not necessarily mean that the insulin infusion commanded by the switched LQG controller will be reduced. If the amount of insulin commanded by the switched LQG is not going to violate the IOB limit, then that amount of insulin is directly infused to the patient without being attenuated.

4. Discussion

A new control strategy for the AP problem was presented: the ARG algorithm. It consists of a two-degree-of-freedom control structure that includes a switched LQG inner controller together with an outer sliding mode safety loop, the SAFE mechanism for IOB constraints. The SAFE layer quickly adapts the controller gain to automatically obtain insulin spikes similar to the open-loop boluses during meal times. It also reduces or suspends the insulin infusion when a risk of hypoglycemia is inferred from the CGM signal. The overall control strategy is simple to migrate to a portable platform, and it was validated in a clinical trial. However, this is an ongoing procedure that can be extended as follows:

- The switched nature of the inner controller enables different tunings for dealing with prandial and fasting periods, and can be extended to other situations, e.g., physical activity.

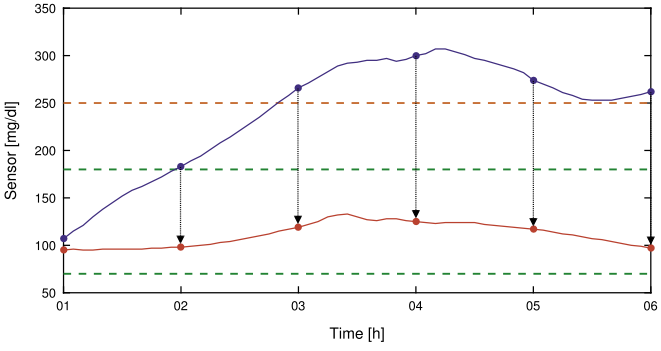

Fig. 9. The ARG control algorithm mitigating the *dawn phenomena*. Clinical response for patient #54116 in open-loop (blue line) and in closed-loop (red line) during the night. Dashed lines (green and orange) represent the limits of the 70–180 mg/dl and 70–250 mg/dl ranges. (For interpretation of the references to color in this figure legend, the reader is referred to the web version of this article.)

- A more general switched-LPV procedure could be considered (Colmegna et al., 2016a). In this work, an LQG strategy was adopted, because it simplified the implementation into a portable platform.

- Unannounced meals, not only carbohydrate counting, can be attempted with an adequate meal detection filter (Turksoy et al., 2016).
- New and more complex scenarios could be potentially addressed by redesigning the switching policy and/or the IOB constraints. For example, the IOB limit could be automatically set based on a carbohydrate estimation algorithm (Samadi et al., 2017).

5. Conclusions

Promising *in silico* and *in vivo* results were obtained using the ARG algorithm without carbohydrate counting, which represent a step forward towards a fully automated AP system.

Acknowledgments

The authors would like to thank the UVA group for its invaluable help to carry out the clinical trials, specially Dr. Daniel Cherñavvsky, and the fruitful conversations with Dr. Ravi Gondhalekar during the development of the ARG algorithm.

The essential collaboration of Roche and Dexcom is also truly appreciated by all authors.

Access to the complete version of the University of Virginia/Padova metabolic simulator was provided by an agreement with Prof. C. Cobelli (University of Padova) and Prof. B. P. Kovatchev (University of Virginia) for research purposes.

References

Atlas, E., Nimri, R., Miller, S., Grunberg, E., & Phillip, M. (2010). MD-Logic artificial pancreas system: A pilot study in adults with type 1 diabetes. *Diabetes Care*, *33*(5), 1072–1076.

Bally, L., Thabit, H., Kojzar, H., Mader, J. K., Qerimi-Hyseni, J., Hartnell, S., et al. (2017). Day-and-night glycaemic control with closed-loop insulin delivery versus conventional insulin pump therapy in free-living adults with well controlled type 1 diabetes: An open-label, randomised, crossover study. *Lancet Diabetes Endocrinol*, *5*(4), 261–270.

Bequette, B. W. (2009). Glucose clamp algorithms and insulin time-action profiles. *Journal of Diabetes Science and Technology*, *3*(5), 1005–1013.

Bequette, B. W. (2012). Challenges and recent progress in the development of a closed-loop artificial pancreas. *Annual Reviews in Control*, *36*(2), 255–266.

Blauw, H., van Bon, A. C., Koops, R., DeVries, J. H., on behalf of the PCDIAB consortium (2016). Performance and safety of an integrated bihormonal artificial pancreas for fully automated glucose control at home. *Diabetes Obesity Metabolism*, *18*(7), 671–677.

Brazeau, A. S., Mircescu, H., Desjardins, K., Leroux, C., Strychar, I., Ekoé, J. M., et al. (2013). Carbohydrate counting accuracy and blood glucose variability in adults with type 1 diabetes. *Diabetes Research and Clinical Practice*, *99*(1), 19–23.

Cameron, F. M., Ly, T. T., Buckingham, B. A., Maahs, D. M., Forlenza, G. P., Levy, C. J., et al. (2017). Closed-loop control without meal announcement in type 1 diabetes. *Diabetes Technology & Therapeutics*, *19*(9), 527–532.

Cameron, F. M., Niemeyer, G., & Bequette, B. W. (2012). Extended multiple model prediction with application to blood glucose regulation. *Journal of Process Control*, *22*(8), 1422–1432.

Chait, A., & Bornfeldt, K. E. (2009). Diabetes and atherosclerosis: Is there a role for hyperglycemia? *The Journal of Lipid Research*, *50*, S335–S339.

Clarke, W., & Kovatchev, B. P. (2009). Statistical tools to analyze continuous glucose monitor data. *Diabetes Technology & Therapeutics*, *11*(Suppl 1), S45–S54.

Colmegna, P., Sánchez-Peña, R. S., & Gondhalekar, R. (2018). Linear parameter-varying model to design control laws for an artificial pancreas. *Biomedical Signal Processing and Control*, *40*, 204–213.

Colmegna, P., Sánchez-Peña, R. S., Gondhalekar, R., Dassau, E., & Doyle III, F. J. (2016a). Reducing glucose variability due to meals and postprandial exercise in T1DM using switched LPV control: In silico studies. *Journal of Diabetes Science and Technology*, *10*(3), 744–753.

Colmegna, P., Sánchez-Peña, R. S., Gondhalekar, R., Dassau, E., & Doyle III, F. J. (2016b). Switched LPV glucose control in type 1 diabetes. *IEEE Transactions on Biomedical Engineering*, *63*(6), 1192–1200.

Dalla Man, C., Micheletto, F., Lv, D., Breton, M. D., Kovatchev, B. P., & Cobelli, C. (2014). The UVA/PADOVA type 1 diabetes simulator: New features. *Journal of Diabetes Science and Technology*, *8*(1), 26–34.

Dassau, E., Bequette, B. W., Buckingham, B., & Doyle III, F. J. (2008). Detection of a meal using continuous glucose monitoring. *Diabetes Care*, *31*(2), 295–300.

Dassau, E., Zisser, H., Harvey, R., Percival, M., Grosman, B., Bevier, W., et al. (2013). Clinical evaluation of a personalized artificial pancreas. *Diabetes Care*, *36*(4), 801–809.

de Bock, M., Roy, A., Cooper, M., Dart, J., Berthold, C., Retterath, A., et al. (2015). Feasibility of outpatient 24-hour closed-loop insulin delivery. *Diabetes Care*, *38*(11), e186–e187.

de Pereda, D., Romero-Vivo, S., Ricarte, B., Rossetti, P., Ampudia-Blasco, F. J., & Bondia, J. (2016). Real-time estimation of plasma insulin concentration from continuous glucose monitor measurements. *Computer Methods and Programs in Biomedicine*, *19*(9), 934–942.

El-Khatib, F. H., Balliro, C., Hillard, M. A., Magyar, K. L., Ekhlaspour, L., Sinha, M., et al. (2017). Home use of a bihormonal bionic pancreas versus insulin pump therapy in adults with type 1 diabetes: A multicentre randomised crossover trial. *Lancet*, *389*(10067), 369–380.

Ellingsen, C., Dassau, E., Zisser, H., Grosman, B., Percival, M., Jovanovič, L., et al. (2009). Safety constraints in an artificial pancreatic β cell: An implementation of model predictive control with insulin on board. *Journal of Diabetes Science and Technology*, *3*(3), 536–544.

Fabris, C., Patek, S. D., & Breton, M. D. (2016). Are risk indices derived from CGM interchangeable with SMBG-based indices? *Journal of Diabetes Science and Technology*, *10*(1), 50–59.

Forlenza, G. P., Deshpande, S., Ly, T. T., Howsmon, D. P., Cameron, F., Baysal, N., et al. (2017). Application of zone model predictive control artificial pancreas during extended use of infusion set and sensor: A randomized crossover-controlled home-use trial. *Diabetes Care*, *40*(8), 1096–1102.

Garelli, F., Mantz, R., & De Battista, H. (2011). *Advanced control for constrained processes and systems*. London, United Kingdom: IET Institution of Engineering and Technology.

Gingras, V., Haidar, A., Messier, V., Legault, L., Ladouceur, M., & Rabasa-Lhoret, R. (2016). A simplified semiquantitative meal bolus strategy combined with single- and dual-hormone closed-loop delivery in patients with type 1 diabetes: A pilot study. *Diabetes Technology & Therapeutics*, *18*(8), 464–471.

Gingras, V., Rabasa-Lhoret, R., Messier, V., Ladouceur, M., Legault, L., & Haidar, A. (2016). Efficacy of dual-hormone artificial pancreas to alleviate the carbohydrate-counting burden of type 1 diabetes: A randomized crossover trial. *Diabetes Metabolism*, *42*(1), 47–54.

Gondhalekar, R., Dassau, E., & Doyle III, F. J. (2014). MPC design for rapid pump-attenuation and expedited hyperglycemia response to treat T1DM with an artificial pancreas. In *AACC American control conference* (pp. 4224–4230), Portland, OR, USA.

Gondhalekar, R., Dassau, E., & Doyle III, F. J. (2016). Periodic zone-MPC with asymmetric costs for outpatient-ready safety of an artificial pancreas to treat type 1 diabetes. *Automatica*, *71*(9), 237–246.

Haidar, A., Messier, V., Legault, L., Ladouceur, M., & Rabasa-Lhoret, R. (2017). Outpatient 60-hour day-and-night glucose control with dual-hormone artificial pancreas, single-hormone artificial pancreas, or sensor-augmented pump therapy in adults with type 1 diabetes: An open-label, randomised, crossover, controlled trial. *Diabetes Obesity Metabolism*, *19*(5), 713–720.

Harvey, R., Dassau, E., Zisser, H., Seborg, D. E., & Doyle III, F. J. (2008). Design of the glucose rate increase detector: A meal detection module for the health monitoring system. *Journal of Diabetes Science and Technology*, *8*(2), 307–320.

Hespanha, J. P., & Morse, A. S. (2002). Switching between stabilizing controllers. *Automatica*, *38*(11), 1905–1917.

Hovorka, R., Elleri, D., Thabit, H., Allen, J., Leelarathna, L., El-Khairi, R., et al. (2014). Overnight closed-loop insulin delivery in young people with type 1 diabetes: A free-living, randomized clinical trial. *Diabetes Care*, *37*(5), 1204–1211.

Hughes, C. S., Patek, S. D., Breton, M. D., & Kovatchev, B. P. (2011). Anticipating the next meal using meal behavioral profiles: A hybrid model-based stochastic predictive control algorithm for T1DM. *Computer Methods and Programs in Biomedicine*, *102*(2), 138–148.

Keith-Hynes, P., Mize, B., Robert, A., & Place, J. (2014). The diabetes assistant: A smartphone-based system for real-time control of blood glucose. *Electronics*, *3*(4), 609–623.

Kovatchev, B. P., Breton, M. D., Dalla Man, C., & Cobelli, C. (2008). In silico model and computer simulation environment approximating the human glucose/insulin utilization. Food and Drug Administration Master File MAF 1521.

Kovatchev, B. P., Breton, M. D., Dalla Man, C., & Cobelli, C. (2009). In silico preclinical trials: A proof of concept in closed-loop control of type 1 diabetes. *Journal of Diabetes Science and Technology*, *3*(1), 44–55.

Kovatchev, B. P., Cheng, P., Anderson, S. M., Pinsker, J. E., Boscari, F., Buckingham, B. A., et al. (2017). Feasibility of long-term closed-loop control: a multicenter 6-month trial of 24/7 automated insulin delivery. *Diabetes Technology & Therapeutics*, *19*(1), 18–24.

Lee, J. B., Dassau, E., Seborg, D. E., & Doyle III, F. J. (2013). Model-Based personalization scheme of an artificial pancreas for type 1 diabetes applications In *American control conference* (pp. 2911–2916), Washington, DC, USA.

León-Vargas, F., Garelli, F., De Battista, H., & Vehi, J. (2015). Postprandial response improvement via safety layer in closed-loop blood glucose controllers. *Biomedical Signal Processing and Control*, *16*, 80–87.

Ly, T., Roy, A., Grosman, B., Shin, J., Campbell, A., Monirabbasi, S., et al. (2015). Day and night closed-loop control using the integrated Medtronic hybrid closed-loop system in type 1 diabetes at diabetes camp. *Diabetes Care*, *38*(7), 1205–1211.

Magni, L., Raimondo, D. M., Dalla Man, C., Breton, M. D., Patek, S. D., De Nicolao, G., et al. (2008). Evaluating the efficacy of closed-loop glucose regulation via control-variability grid analysis. *Journal of Diabetes Science and Technology*, *2*(4), 630–635.

Messori, M., Kropff, J., Del Favero, S., Place, J., Visentin, R., Calore, R., et al. (2017). Individually adaptive artificial pancreas in subjects with type 1 diabetes: A one-month proof-of-concept trial in free-living conditions. *Diabetes Technology & Therapeutics*, *19*(10), 560–571.

Patek, S. D., Magni, L., Dassau, E., Hughes-Karvetski, C., Toffanin, C., De Nicolao, G., et al. (2012). Modular closed-loop control of diabetes. *IEEE Transactions on Biomedical Engineering*, *59*(11), 2986–2999.

Phillip, M., Battelino, T., Atlas, E., Kordonouri, O., Bratina, N., Miller, S., et al. (2013). Nocturnal glucose control with an artificial pancreas at a diabetes camp. *New England Journal of Medicine*, *368*(9), 824–833.

Reddy, M., Herrero, P., Sharkawy, M. E., Pesl, P., Jugnee, N., Pavitt, D., et al. (2015). Metabolic control with the bio-inspired artificial pancreas in adults with type 1 diabetes: A 24-hour randomized controlled crossover study. *Journal of Diabetes Science and Technology*, *10*(2), 405–413.

Renard, E. (2008). Insulin delivery route for the artificial pancreas: Subcutaneous, intraperitoneal, or intravenous? Pros and cons. *Journal of Diabetes Science and Technology*, *2*(4), 735–738.

Revert, A., Garelli, F., Picó, J., De Battista, H., Rossetti, P., Vehi, J., et al. (2013). Safety auxiliary feedback element for the artificial pancreas in type 1 diabetes. *IEEE Transactions on Biomedical Engineering*, *60*(8), 2113–2122.

Safonov, M. G., & Chiang, R. Y. (1989). A Schur method for balanced-truncation model reduction. *IEEE Transactions on Automatic Control*, *34*(7), 729–733.

Samadi, S., Turksoy, K., Hajizadeh, I., Feng, J., Sevil, M., & Cinar, A. (2017). Meal detection and carbohydrate estimation using continuous glucose sensor data. *IEEE Journal of Biomedical and Health Informatics*, *21*(3), 619–627.

Sánchez-Peña, R. S., Colmegna, P., Grosembacher, L., Breton, M. D., De Battista, H., Garelli, F., et al. (2017). Artificial pancreas: First clinical trials in Argentina. In *20th IFAC world congress* (pp. 7997–8002), Toulouse, France.

Steil, G. M., Panteleon, A. E., & Rebrin, K. (2004). Closed-loop insulin delivery-the path to physiological glucose control. *Advanced Drug Delivery Reviews*, *56*(2), 125–144.

Steil, G. M., Rebrin, K., Darwin, C., Hariri, F., & Saad, M. F. (2006). Feasibility of automating insulin delivery for the treatment of type 1 diabetes. *Diabetes*, *55*(12), 3344–3350.

Szalay, P., Eigner, G., & Kovács, L. A. (2014). Linear matrix inequality-based robust controller design for type-1 diabetes model. In *19th IFAC world congress* (pp. 9247–9252), Cape Town, South Africa.

The Diabetes Control and Complications Trial Research Group (1997). Hypoglycemia in the diabetes control and complications trial. *Diabetes*, *46*(2), 271–286.

Turksoy, K., Hajizadeh, I., Samadi, S., Feng, J., Sevil, M., Park, M., et al. (2017). Real-time insulin bolusing for unannounced meals with artificial pancreas. *Control Engineering Practice*, *59*(Supplement C), 159–164.

Turksoy, K., Samadi, S., Feng, J., Littlejohn, E., Quinn, L., & Cinar, A. (2016). Meal detection in patients with type 1 diabetes: A new module for the multivariable adaptive artificial pancreas control system. *IEEE Journal of Biomedical and Health Informatics*, *20*(1), 47–54.

van Heusden, K., Dassau, E., Zisser, H. C., Seborg, D. E., & Doyle III, F. J. (2012). Control-relevant models for glucose control using *a priori* patient characteristics. *IEEE Transactions on Biomedical Engineering*, *59*(7), 1839–1849.

Vinnicombe, G. (1993). Frequency domain uncertainty and the graph topology. *IEEE Transactions on Automatic Control*, *38*(9), 1371–1383.

Vinnicombe, G. (2001). *Uncertainty and feedback: $\mathcal{H}_\infty$ loop-shaping and the ν-gap metric*. London: Imperial College Press.

Visentin, R., Dalla Man, C., Kovatchev, B. P., & Cobelli, C. (2014). The University of Virginia/Padova type 1 diabetes simulator matches the glucose traces of a clinical trial. *Diabetes Technology & Therapeutics*, *16*(7), 428–434.

Walsh, J., & Roberts, R. (2006). *Pumping insulin* (4th ed.). Torrey Pines Press, San Diego, CA.

Walsh, J., Roberts, R., & Heinemann, L. (2014). Confusion regarding duration of insulin action: A potential source for major insulin dose errors by bolus calculators. *Journal of Diabetes Science and Technology*, *8*(1), 170–178.

Weinzimer, S. A., Steil, G. M., Swan, K. L., Dziura, J., Kurtz, N., & Tamborlane, W. V. (2008). Fully automated closed-loop insulin delivery versus semiautomated hybrid control in pediatric patients with type 1 diabetes using an artificial pancreas. *Diabetes Care*, *31*(5), 934–939.

Willinska, M. E., Chassin, L. J., Schaller, H. C., Schaupp, L., Pieber, T. R., & Hovorka, R. (2005). Insulin kinetics in type 1 diabetes: Continuous and bolus delivery of rapid acting insulin. *IEEE Transactions on Biomedical Engineering*, *52*(1), 3–12.

Youla, D. C., Jabr, H. A., & Bongiorno, J. J. (1976). Modern wiener-hopf design of optimal controllers–part ii: The multivariable case. *IEEE Transactions on Automatic Control*, *21*(3), 319–338.